

# Optimization measurement of hydrogen gas concentration by using high accuracy TDLAS

Alifu Xiafukaiti<sup>(a, b)</sup>, Nofel Lagrosas<sup>(b, c)</sup>, Masakazu Ogita<sup>(d)</sup>, Nobuhiko Oi<sup>(d)</sup>, Yuji Ichikawa<sup>(d)</sup>, Sachiyo Sugimoto<sup>(d)</sup>, Ipppei Asahi<sup>(d)</sup>, Shigeru Yamaguchi<sup>(e)</sup>, Tatsuo Shiina<sup>(b)</sup>

<sup>(a)</sup> Information Technology R&D Center, Mitsubishi Electric Corporation, 5-1-1, Ofuna, Kamakura-shi, Kanagawa, Japan

<sup>(b)</sup> Graduate School of Engineering, Chiba University, 1-33, Yayoicho, Inage-ku, Chiba-shi, Chiba, Japan

<sup>(c)</sup> School of Engineering, Kyushu University, Fukuoka-shi, Fukuoka, Japan

<sup>(d)</sup> Shikoku Research Institute inc., 2109-8, Yashimanishimachi, Takamatsu-shi, Kagawa, Japan

<sup>(e)</sup> Tokai University, 4-1-1 Kitakaname, Hiratsuka-shi, Kanagawa, Japan  
*Xiafukaiti.Alifu@ct.MitsubishiElectric.co.jp*

**Abstract:** Trace gas measurement is crucial for maintaining safety, quality control, and environmental protection across various industries. Tunable diode laser absorption spectroscopy (TDLAS) is frequently used for trace gas analysis due to its superior sensitivity and selectivity. However, the measurement of low concentrations of hydrogen gas using TDLAS presents challenges due to its lower absorbance compared to gases such as CO<sub>2</sub>, CH<sub>4</sub>, and NH<sub>3</sub>. In this study, we carried out laboratory-based experiments to evaluate a novel optimal method for detecting hydrogen gas, with the aim of facilitating remote sensing and establishing a foundation for lidar applications. By adjusting the gas cell pressure and line width, we optimized the center wavelength lock and the stable modulation of DFB-laser control. Further optimization involved maximizing the wavelength modulation spectroscopy signals through the careful selection of modulation parameters. This optimal method achieved a detection limit of 100 ppm with integration times of 30 seconds, while the stabilization of our TDLAS system exhibited a fluctuation of 55 ppm.

## 1. Introduction

Hydrogen gas (H<sub>2</sub>) plays a pivotal role in the field of fuel cells and hydrogen energy, necessitating precise measurement of its concentration and quality [1-3]. However, its detection is challenging due to its lightness, colorlessness, and odorlessness. Differential absorption lidar and Raman lidar are two representative lidar techniques currently utilized for gas leak detection [4,5]. In the context of H<sub>2</sub> detection, Raman type lidar has seen significant advancements in H<sub>2</sub> detection technology [6], with a detection limit of 500 ppm H<sub>2</sub> released into the atmosphere measured successfully within 11 minutes. Given H<sub>2</sub>'s high combustion speed, H<sub>2</sub> leak detectors must respond swiftly even at low gas concentrations and trigger an alarm. A key challenge lies in the development of lidar remote sensing capable of detecting H<sub>2</sub> at low concentrations with a rapid response time. This study focuses on practical H<sub>2</sub> leak detection and optimizes tunable diode laser absorption spectroscopy (TDLAS) [8,9]

for enhanced sensitivity, resolution, and real-time measurement. Recently, a novel gas imager employing single-photon lidar with TDLAS has been reported [7], capable of detecting leaks as low as 700 ppm m. However, the combination of a lidar system with TDLAS for H<sub>2</sub> leak detection has not been reported yet. This report discusses the optimization of TDLAS measurement methods to enable the detection of trace amounts of H<sub>2</sub> and the evaluation of H<sub>2</sub> purity, facilitating measurements across a broad concentration range.

## 2. Methodology

Our optimization approach is constructed by implementing a calibration-free method [10], analyzing the characteristics of the absorption line, adjusting laser wavelength modulation, and employing two different optical gas cells. Here, the calibration-free method used is based on the normalization of the second-harmonic signal,  $I_{2f}$ , with first-harmonic signal,  $I_f$ , derived from TDLAS measurement. This normalization

mitigates the effects of unknown or fluctuating optical properties of the light source output and opto-electrical devices. It facilitates the extraction of absorption information, such as gas concentration, from the ratio  $I_{2f}/I_f$  as shown in Equation (1) to (3) below:

$$I_f = I_0 A_0 m \quad (1)$$

$$I_{2f} = I_0 A_0 k_2 \alpha_0 l C \quad (2)$$

$$\frac{I_{2f}}{I_f} = \frac{k_2 \alpha_0 l C}{m} \quad (3)$$

where  $I_0$  and  $m$  represent the incident intensity and intensity modulation index due to the laser current modulation, respectively.  $A_0$  signifies the receiver efficiency factor. The  $\alpha_0$ ,  $l$ , and  $C$  correspond to the absorption coefficient at the absorption center wavelength, optical path length, and gas concentration, respectively. This pioneering calibration-free method enhances the accuracy and reliability of  $H_2$  measurements, thereby promoting the evolution of TDLAS methodologies [11,12].

**Table 1. Value of  $\alpha_0$  and FWHM at different pressures setting.**

Pressure (atm)	$\alpha_0$ ( $m^{-1}ppm^{-1}$ )	FWHM (pm)
0.2	$13.0 \times 10^{-10}$	11.9
0.4	$9.4 \times 10^{-10}$	15.0
0.6	$7.3 \times 10^{-10}$	18.5
0.8	$5.8 \times 10^{-10}$	22.2
1.0	$4.8 \times 10^{-10}$	26.1

Depending on the absorption information from the high-resolution transmission molecular absorption database (HITRAN) [13], a  $H_2$  absorption line at 2121.8 nm within the mid-infrared band is chosen due to its high absorption coefficient and minimal interference from other gases such as  $N_2$ ,  $CO_2$  and  $CH_4$ . The intensity or width of the absorption line also undergoes changes during variations in pressure. To analyze the characteristics of absorption line, the variations in the half-width at half-maximum (HWHM),  $\gamma$ , and  $\alpha_0$  of the  $H_2$  absorption line under different pressures at constant temperature are simulated using HITRAN, with results presented in Table 1. outcomes suggest that the impact of a broader FWHM compared to a reduced  $\alpha_0$  during pressure broadening is more significant in TDLAS measurement as it does not necessitate

a narrow laser line width such as several picometers (pm). So, the cell pressure of the target gas in the experiment is set at 1 atm.

Considering the interaction between the wavelength modulation width,  $\Delta\lambda$ , and the intensity modulation index,  $m$ , attributable to the laser diode's properties, its essential to ascertain the absorption properties of the gas to achieve gas concentration that closely align with actual values. The absorption coefficient,  $\alpha(\lambda)$ , of a Lorentzian line shape is expanded by a Fourier series as given in Equation (4):

$$\alpha(\lambda) = \alpha_0 [k_0 - k_2 \cos(2\pi \times 2ft) + \dots] \quad (4)$$

where  $\gamma$  is the HWHM of the absorption line. The analytical expression of  $k_2$  in Equation (4) was provided by Wahlquist [14]:

$$k_2 = \frac{2[2 + x^2 - 2\sqrt{(1 + x^2)}]}{x^2 \sqrt{(1 + x^2)}} \quad (5)$$

where we define  $x$  as  $\Delta\lambda / \gamma$ . Thanks to the calibration-free method, which eliminates intensity fluctuations arising from factors other than gas absorption, gas concentrations in the ppm order can be measured using the relational expression of  $k_2 / x$ . The value of  $x$  can be adjusted to maximize  $I_{2f} / I_f$ . The maximum is achieved when  $d(k_2/x)/dx = 0$ , yielding a scale factor value of  $x = 0.931$  at  $k_2 / x = 0.243$  [10]. Thus, the optimal modulation width of the laser wavelength at 1 atm is  $\pm 21.3$  pm ( $\Delta\lambda = \gamma x$ ).

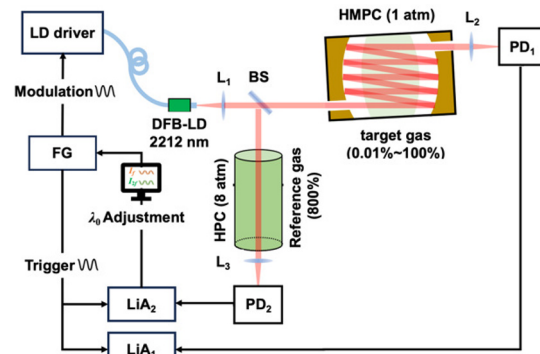


**Figure 1. Experiment configuration for optimizing  $H_2$  detection with low concentrations using TDLAS System.**

Figure 1 shows the experimental setup for measuring  $H_2$  concentration. A distributed feedback laser diode (DFB-LD) emitting near 2122 nm is employed. The DFB-LD, operating at a maximum output power of 5 mW under optimal temperature and injection current settings, maintains a stable temperature around

23°C with an accuracy of 0.1°C to establish the near-locking wavelength of the laser. The DFB-LD has a linear relationship between the injection current and both the center wavelength and output power. Its optical properties such as wavelength and output shifts are approximately 20 pm and 0.82 mV per mA, respectively. The LD output power, measured in mV units, is recorded by photodiode (PD), facilitating the adjustment of modulation width in TDLAS measurements. These optical properties render the DFB-LD suitable for H<sub>2</sub> measurement using our TDLAS method. The DFB-LD frequency is sinusoidally modulated at  $f = 10$  kHz, with the modulation center locked to the center of the maximum absorption line of H<sub>2</sub> ( $\lambda = 2121.83$  nm). The collimated laser beam is split by a beam splitter (BS), and the transmitted beam enters a Herriott multipass cell (HMPC) with an optical length of 10.43 m, filled with the target gas. The attenuated laser beam, after multiple reflections from the HMPC, is focused by a second lens into PD<sub>1</sub>. PD<sub>1</sub> detects the attenuated laser beam, feeding the lock-in amplifier 1 (LiA<sub>1</sub>) to record  $I_{f\text{-target}}$  and  $I_{2f\text{-target}}$  from H<sub>2</sub> absorption in the HMPC. The beam reflected from BS traverses a high-pressure cell (HPC) with an optical length of 0.7 m. The HPC, filled with reference gas at a pressure of 8 atm, detects the component of the attenuated laser beam through PD<sub>2</sub>, which is then fed into the LiA<sub>2</sub> to record  $I_{f\text{-reference}}$  and  $I_{2f\text{-reference}}$  from H<sub>2</sub> absorption in the HPC. The center wavelength of the DFB-LD is adjusted to achieve a known ratio between  $I_{f\text{-reference}}$  and  $I_{2f\text{-reference}}$ , calculated from Equation (3) using setting parameters such as  $\alpha_0$ ,  $l$ ,  $C$ ,  $m$ , and  $k_2$ .

### 3. Results and Discussions

In the experiment, the gas mixtures are generated using pure H<sub>2</sub> (concentration of 100%), a blend of H<sub>2</sub> (4%) and nitrogen gas (N<sub>2</sub>) (96%), and pure N<sub>2</sub> (concentration of 100%). The HMPC is filled with mixed gases containing H<sub>2</sub> concentrations of 100, 80, 60, 40 and 20%, mixed by adjusting the pressure to 1 atm using pure H<sub>2</sub> and pure N<sub>2</sub>, with the balance of pressure at 1 atm. Additionally, H<sub>2</sub> concentrations of 4, 1, 0.4, 0.1, 0.04, 0.01, and 0.004% are achieved by mixing a blend of H<sub>2</sub> (4%) and pure N<sub>2</sub> (100%) with the balance of pressure at 1 atm. For the reference gas in the HPC, pure H<sub>2</sub> is injected at a pressure of 8 atm. Figures 2 (a) and (b) show the recorded signals

over measurement time and its average value of  $I_{2f\text{-target}} / I_{f\text{-target}}$  with related concentration. As the value of  $I_{2f\text{-target}}$  decreases with decreasing concentration, the ratio of two harmonic signals are decreases. The fluctuation of these signals results in noticeable variations due to the short time constant of 1 second employed in the measurement process. Moreover, these variations can be attributed to the precision limitations of the laser driver and function generator for LD modulation used in the experiment. Therefore, to mitigate such fluctuations, strategies such as employing a longer time constant or utilizing more accurate laser drivers and function generators could be adopted. However, implementing these solutions may either extend the measurement process or increase the overall system cost. These data points are linearly fitted using the equation  $y = 1.3 \times 10^{-5}x$ , with a coefficient of determination ( $R^2$ ) value calculated as 0.9995. However, the average value of  $I_{2f\text{-target}} / I_{f\text{-target}}$  at a concentration of 0.004% (40 ppm) demonstrates non-linearity, marking the threshold of measurement capability.

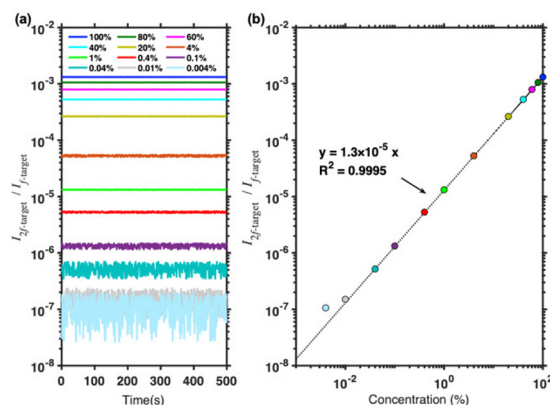


Figure 2. Changes in (a) row and (b) average values of  $I_{2f\text{-target}} / I_{f\text{-target}}$  at different concentration.

To evaluate the measurement precision and long-term stability of our method, the HMPC is filled with 100% H<sub>2</sub>, and data are collected over a span of 2500 seconds with a 100-millisecond interval, as shown in Fig. 3(a). The resulting Allan deviation is illustrated in Fig. 3(b). The minimum detection limit without integration (0.1 second) is 3% (30000 ppm), and as the integration time increase, the minimum detection limits decrease. As a result, the minimum detection limits reach 0.2866% (2866 ppm) and 0.0055% (55 ppm) at integration times of 1 second and 30 seconds, respectively.

However, beyond an integration time of 30 seconds, the minimum detection limits begin to increase.

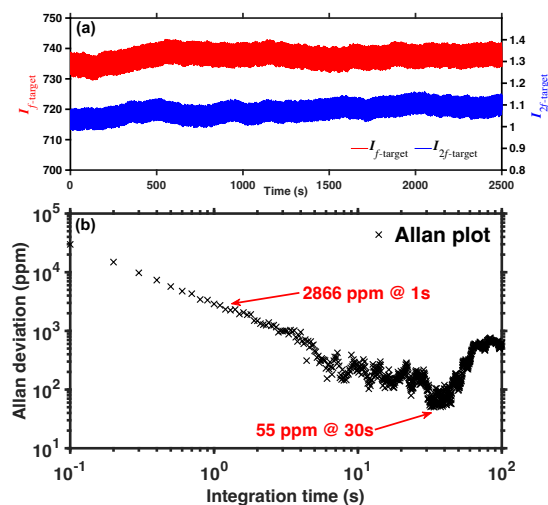


Figure 3. Temporal variation of (a)  $I_{2f-target}$  and  $I_{f-target}$  values, and deviation of measured concentration over varying integration times resulting from Allan deviation.

#### 4. Summary

The findings of this study underscore the efficacy of TDLAS in quantifying measurement of  $H_2$  concentration. The key insights and conclusions, which incorporate HITRAN simulations, indicate that controlling the gas cell pressure and TDLAS modulation width can successfully facilitate precise quantitative measurement of  $H_2$  gas. This effectively demonstrates the versatility of the method, resulting in accurate measurements of  $H_2$  concentration ranging from 0.01% to 100%. The study uncovers a correlation between integration time and minimum detection limits. While a minimum detection limit of 3% is observed at 0.1 seconds integration, this limit decreases to 0.0055% at 30 seconds of integration time, underscoring the impact of integration time on measurement precision. Beyond 30 seconds of integration time, an increase in minimum detection limits is observed. This phenomenon can be attributed to factors such as optical elements, DFB-LD's line width, and noise of PD, emphasizing the importance of considering system limitations. The calibration method employed ensures the method's adaptability to a wide range of concentrations. In future, our method holds potential applications in lidar techniques for precise  $H_2$  gas measurement, which could be beneficial for trace gas sensing in  $H_2$  gas

stations or vehicles. Additionally, it could be utilized for quality checks of  $H_2$ .

#### 5. References

- [1] F. Zhang, et al., "The survey of key technologies in hydrogen energy storage," *Int J Hydrogen Energy* **41**(33), 14535-14552 (2016).
- [2] M. Hirscher, et al., "Materials for hydrogen-based energy storage: a past, recent progress and future outlook," *J Alloys and Comps* **827**, 153548 (2020).
- [3] T. Shimizu, et al., "A region-specific environmental analysis of technology implementation of hydrogen energy in Japan based on life cycle assessment," *J Ind Ecol* **24**(1), 217-33 (2020).
- [4] F. Innocenti, et al., "Differential Absorption Lidar (DIAL) Measurements of Landfill Methane Emissions," *Remote Sens* **9**(9), 953 (2017).
- [5] T. Somekawa, et al., "Flash resonance Raman lidar for  $SO_2$  gas leak detection," *Opt Commun* **513**, 128083 (2022).
- [6] A. Liméry, et al., "Raman lidar for hydrogen gas concentration monitoring and future radioactive waste management," *Opt Express* **25**(24), 30636-30641 (2017).
- [7] J. Titchener, et al., "Single photon Lidar gas imagers for practical and widespread continuous methane monitoring," *Appl Energy* **306**(B), 118086 (2022).
- [8] E. D. Hinkley, "High-Resolution Infrared Spectroscopy with a Tunable Diode Laser," *Appl Phys Lett* **16**(9), 351-354 (1970).
- [9] J. Reid and D. Labrie, "Second-harmonic detection with tunable diode lasers - Comparison of experiment and theory," *Appl Phys B Photophys Laser Chem* **26**(3), 203-210 (1981).
- [10] T. Iseki, et al., "A portable remote methane sensor using a tunable diode laser," *Meas Sci Technol* **11**(6), 594-602 (2000).
- [11] G. B. Rieker, et al., "Calibration-free wavelength-modulation spectroscopy for measurements of gas temperature and concentration in harsh environments," *Appl Opt* **48**(29), 5546-5560 (2009).
- [12] J.N. Oliaee, et al., "Development of a Sub-ppb resolution methane sensor using a GaSb-based DFB diode laser near 3270 nm for fugitive emission measurement," *ACS Sens* **7**(2), 564-572 (2022).
- [13] I. E. Gordon, et al., "The HITRAN 2020 molecular spectroscopic database," *J Quant Spectrosc Radiat Transf* **277**, 107949 (2022).
- [14] H. Wahlquist "Modulation broadening of unsaturated Lorentzian lines," *J Chem Phys* **35**, 1708-1710 (1961).